NUMERICAL INVESTIGATIONS OF PARALLEL BVI NOISE WITH SPLIT TIP VORTICES

Chi-Hoon Cho
Graduate Student

Duck-Joo Lee
Professor

Department of Aerospace Engineering, KAIST, KOREA

Changjeon Hwang
Senior Researcher
Rotorcraft Development Division, KARI, KOREA

ABSTRACT

To reduce the helicopter blade-vortex interaction(BVI) noise, various efforts have been pursued for 20 years or so. One of the passive methods is using a split tip vortex. There are several studies on such a kind of concept using the vortex wake model. In this study, two dimensional CFD model is used to investigate the detailed flow dynamics for parallel interaction of a blade and split vortices. High-order compact scheme with optimized coefficients is employed for the simulation since it exhibit little numerical dissipation and dispersion error for vorticity and acoustic waves. From the simulation results importance of miss-distances between blade and vortices is emphasized. It is also shown that the BVI with split-vortices can be decomposed into individual interactions of each vortex with the miss-distance modified by co-rotation of the vortices.

INTRODUCTION

The blade-vortex interaction(BVI) occurs on rotorcrafts such as helicopter and tilt rotor when a rotor blade passes close to vortex filament previously trailed at the tip of rotor blades. This interaction causes significant noise problems. For example, despite of their versatility, helicopters' BVI noise is one of the major limitations in broadening their use for civil transportation.

Various reduction methods for BVI noise are proposed(Ref.11), which are based on the ideas of i) weakening tip vortex, ii) separating vortex with blade and iii) controlling aerodynamics during interaction and so on. The reduction methods also can be classified as passive techniques(such as shape modification of airfoil, blade, tip etc.), active techniques(such as higher harmonic control, individual blade control, active flap, etc.) and flight path technique (avoiding high-BVI generating conditions)(Ref.4).

One of the tip shape modification methods is to split the tip vortex into two separate co-rotating cores of nearly equal half strength by using sub-wing tip or vane tip shown in Fig.1. Several studies about this split(or twin) vortex method were reported. Brocklehurst et al.(Ref.1) studied that the noise reduction effect of rectangular vane tip wing experimentally. Brand(Ref.3) studied the characteristics of split vortices generated at sub-wing tip numerically. Beddoes et al.(Ref.2) calculated a high resolution airload of the rectangular vane tip using Beddoes' 3rd generation wake model, and predicted the BVI noise using chordwise compact FW-H code so called DEAF. Hwang et al.(Ref.5) expanded the concept of rectangular vane tip to BERP tip and then performed the parametric study for BERP vane tip, so called KBERP using Beddoes' wake model.

In this study, two dimensional CFD model is used to investigate parallel interaction of blade and split vortices. Although two dimensional model cannot simulate the whole rotor flow, it does simulate the detailed flow dynamics during parallel BVI, better than the wake model. Single vortex case is simulated as preliminary study, then several cases of split vortices are studied.

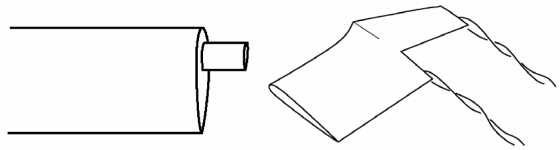

(a) (b)

Fig.1 Blade tip shapes generating split vortices (a) sub-wing tip (b) vane tip

Presented at the 62nd Annual Forum of American Helicopter Society International, Phoenix, Arizona, May 9-11, 2006.

NUMERICAL SOLUTION PROCEDURE

The governing equations are unsteady compressible Euler equations. The equations are written in two dimensional conservative form and in a computational domain as,

$$\frac{\partial \hat{\mathbf{Q}}}{\partial t}+\frac{\partial \hat{\mathbf{E}}}{\partial \xi}+\frac{\partial \hat{\mathbf{F}}}{\partial \eta}=0$$
$$\hat{\mathbf{Q}}=\mathbf{Q}/J$$
$$\hat{\mathbf{E}}=(\xi_x\mathbf{E}+\xi_y\mathbf{F})/J$$
$$\hat{\mathbf{F}}=(\eta_x\mathbf{E}+\eta_y\mathbf{F})/J$$

Description of the variables is in many textbooks or papers.

High-order finite difference compact scheme are used to evaluate the flux derivatives on a structured grid. Fourth-order penta-diagonal seven-point stencil type of central compact scheme with optimized coefficients for minimum dispersion error is used on interior node, and biased or one-sided compact schemes also with optimized coefficients in the same manner are used on the boundary and near-boundary nodes(Ref.6). Time-marching procedure is done by explicit, linear fourth-order Runge-Kutta scheme. To remove unwanted numerical oscillations, adaptive artificial dissipation is added at the last stage of the Runge-Kutta scheme(Ref.8). These high-order and high-resolution schemes exhibit little dissipation and dispersion of vorticity and acoustic waves.

In BVI calculation, incident vortices are placed in front of an airfoil. Scully vortex model is used as velocity profile. The velocity increases linearly with distance in the core and decreases with inverse of distance in the far region. Density and pressure drop of the vortex are calculated from radial directional momentum equation and uniform total enthalpy relation. The vortex flow quantities are superimposed on the steady flow around the airfoil as the initial condition of BVI calculation.

Grid system shown in Fig.2 consists of one airfoil-fitted block and eight blocks surrounding it. This configuration has the advantage to get high grid density in the vortex path area. In the calculation, 7.5 grid points resolve the vortex core diameter, resulting that only 3% of maximum tangential velocity is dissipated after convection of 100 times core diameter distance with Mach 0.5 speed.

Generalized characteristic boundary conditions are used to impose the time-dependent conditions of primitive or characteristic variables at airfoil wall, inflow and outflow boundary, and all interface boundaries between adjacent blocks (Ref.7, 9).

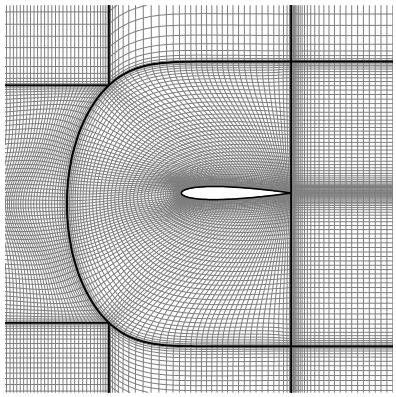

Fig.2 Grid system

BVI WITH SINGLE VORTEX

Preliminarily the aspect of BVI with single vortex is studied. Simulation conditions are listed in Table.1. Freestream velocity and strength(circulation) of the incident vortex follows the realistic parallel BVI condition of four-bladed Super Linx helicopter at approach-to-landing flight. Only initial vertical distance of vortex core from airfoil chord-line is varied in the simulations of three cases; *vortex impinging*, *skimming* and *passing at a distance*. Simulation conditions are listed in Table 1.

Airfoil (NACA0012)	
AoA	0 deg.
Freestream speed	0.5
Vortex (Scully model)	
Strength	-0.13 (counter-clockwise)
core radius	0.05
initial x position	-4.5
initial y position	0.00 impinging -0.20 skimming -0.50 passing at a distance

(non-dimensionalized by sound speed and airfoil chord length)

Table 1. Simulation conditions for BVI with single vortex

Aerodynamic fluctuation

Incident vortex in far upwind region affects airfoil as slowly varying downwash. When the vortex nears the airfoil, aerodynamic forces fluctuate with time as shown in Fig.4. The most significant fluctuation occurs impulsively near the time 0. Fig.5 shows distribution of maximum value of time derivative of surface pressure. Fluctuation of surface pressure is dominant near the leading edge. In other words,

aerodynamic fluctuation during BVI is highly localized spatially in the leading edge region and temporally at the time vortex passes below the region (Ref.10). Then, the miss-distance can be rigorously defined as the minimum distance between leading edge and vortex core trajectory, and it is the key parameter of BVI.

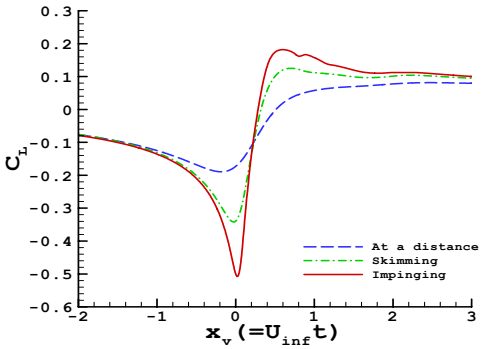

(a)

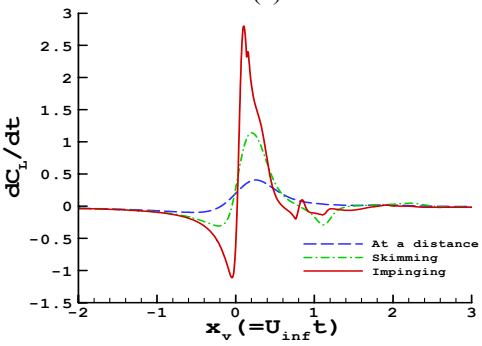

(b)

Fig.4 Fluctuation of aerodynamic force (a) lift coefficient (b) time derivative of lift coefficient

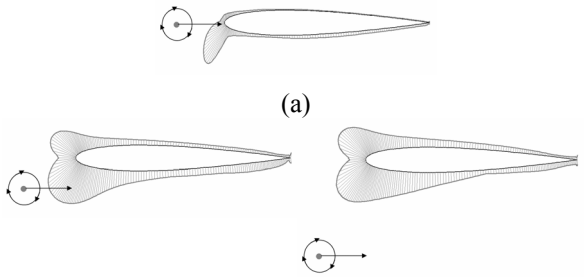

(a)

(b) (c)

Fig.5 Distribution of maximum value of time derivative of surface pressure (a) *passing at a distance* (b) *skimming* (c) *impinging*

Noise radiation

Acoustic wave generated by BVI is directly calculated. Fig.6 shows directional pattern of maximum peak value of acoustic pressure at chord 5 length distance from leading edge in airfoil fixed coordinate. Fig.6 shows the contours of pressure perturbed from steady solution without incident vortex. For impinging case, more intense noise propagates in lower side than upper side, like surface pressure distribution. Those can be explained by the acoustic analogy, which says that the far-field level of acoustic wave is approximately proportional to the time derivative of lift force.

Noise generation and propagation patterns can be viewed more precisely by snapshots of perturbed pressure field from steady solution, of time 5, shown in Fig.7. For *impinging* case Fig.7(a), intense impulsive wave is radiated at compact region near leading edge, and weak impulsive wave at trailing edge. It is observed that directional lobes are at about angles of $\pm\sin(M)$ in ground fixed coordinate.a

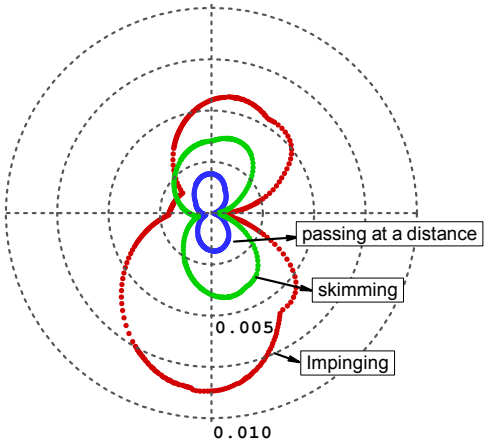

Fig.6 Directional pattern of maximum peak value of acoustic pressure at chord 5 length distance

BVI WITH SPLIT VORTICES

The features of BVI with split-vortices are i) co-rotation of the vortices and ii) multiple interactions occurring simultaneously or in short time interval. These cause the different configuration from single vortex interaction. From the simulations of strong BVI, characteristics of BVI with split vortices are studied.

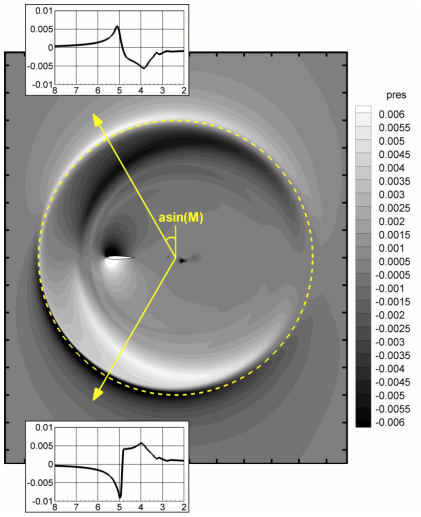

(a)

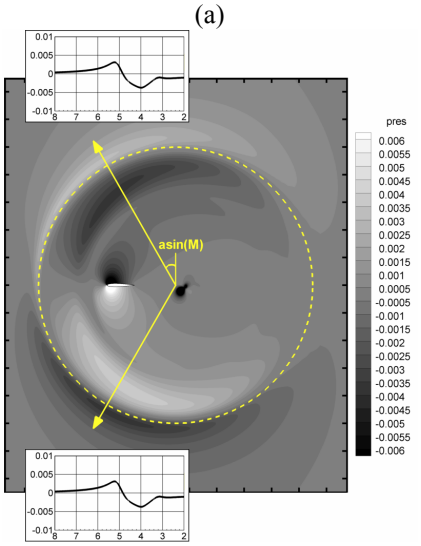

(b)

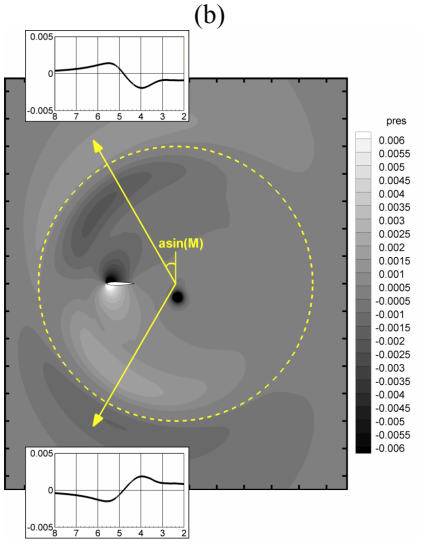

(c)

Fig.7 Contours of pressure field perturbed from steady solution, at time 5 (a) *impinging* (b) *skimming* (c) *passing at a distance*

Simulation of strong BVI conditions

The configuration of two vortices depends mainly on i) vane tip design which could change vortex separation distance, co-rotation speed and so on, and ii) flight condition which could change miss-distance. Because all cases cannot be covered, in this study representative two cases in strong BVI conditions are selected and simulated; 1) *double impinging*, 2) *both-sides skimming*. Vortex positions of these cases are shown in Fig.8(three dimensional position in rotor) and Fig.9(two dimensional position in chord-wise plane). Split vortices are assumed to have the equal core size and strength. By conservation of total strength of trailing vortices (Ref.3), strength of each vortex is set to one half that of single tip vortex. Separation distance between two vortices is set to six times core radius distance that is 30% chord length, which is quite short distance compared with the actual one to make severe condition. Co-rotation speed of vortex cores is 0.0671, which is 13% of freestream speed. The simulation conditions are listed in Table 2.

As shown in Fig.10, both of split cases shows lower fluctuation level than *impinging with single vortex*. *Double impinging* case has two large plus peaks in time derivative of lift. The peaks are caused by the two vortices respectively. For *both-sides skimming*, two vortices interacts with blade instantaneously, thus only one large peak is shown.

Split Vortices	
separation distance	0.30 (6 times core size radius)
strength	-0.065 (co-rotating speed=0.0671)
Initial positions (x, y)	double impinging (-4.4124285,0.12607967) (-4.2875715,-0.14670367) both-sides skimming (-4.6317653,-0.07167913) (-4.3682347,0.07167913)

Table 2 Simulation conditions for blade-split vortices interaction

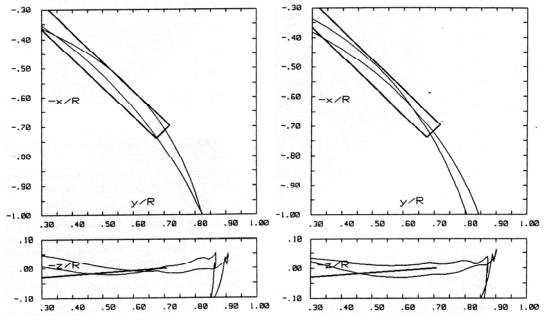

(a) (b)

Fig.8 Wake geometry for split vortices (Ref.2) (a) *double impinging* (b) *both-sides skimming*

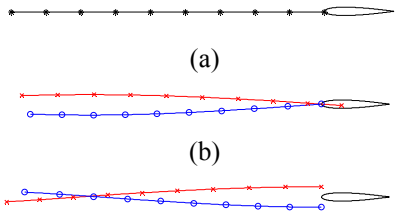

(a)

(b)

(c)

Fig.9 Approach trajectory of split vortices in chord-wise plane(a) *single impinging* (b) *double impinging* (c) *both-sides skimming*

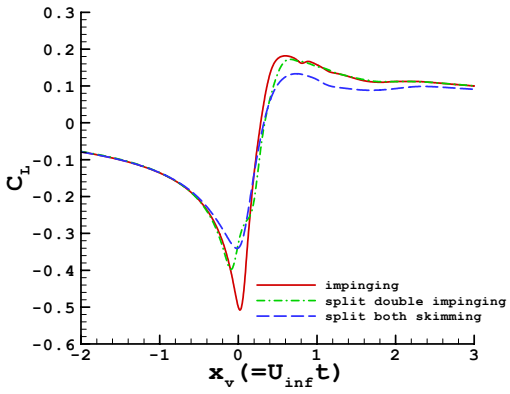

(a)

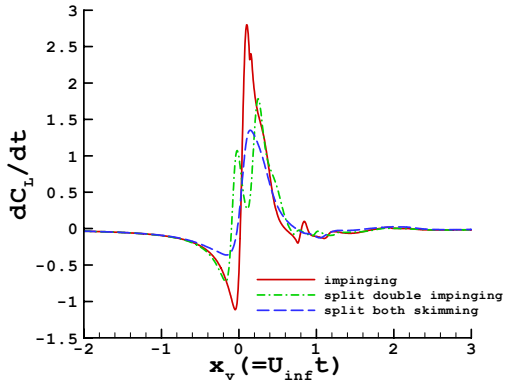

(b)

Fig.10 Comparison of lift fluctuations for single vortex and split vortices (a) lift coefficient (b) time derivative of lift coefficient

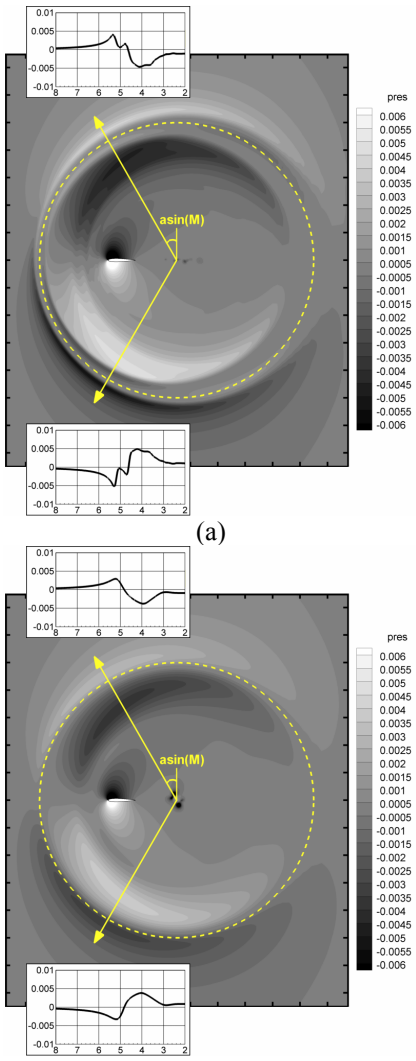

(a)

(b)

Fig.11 Contours of pressure field perturbed from steady solution, at time 5 (a) *double impinging* (b) *both-sides skimming*

Decomposition of split-vortices interaction

It is reminded that BVI is governed by only localized region and time, and the miss-distance defined rigorously is the key parameter of BVI. This means that whether the vortex co-rotates or not, and whether multiple interactions occurs simultaneously or not, BVIs with the same miss-distance would result in the same aerodynamics. Based on this, decomposition analysis is conducted, with the procedure as shown in Fig.10; 1) co-rotating two vortices are decomposed into one by one and 2) the initial positions of each vortex are modified to have the same miss-distances with original case, 3) then the decomposed cases are simulated and 4) finally their aerodynamic fluctuations are summed. Simulation conditions for the decomposed *double impinging* and *both-sides skimming* are listed in Table 3.

For lift fluctuation, the decomposition simulation agrees very well with the original case shown in Fig.13 and Fig.14. Because BVI noise is highly correlated with lift fluctuation, the decomposition simulation is also effective for noise.

From the decomposability of multiple vortices, various cases of blade-split vortices interaction can

be calculated as individual blade-single vortex interaction, with consideration of co-rotation rate and separation distance of the vortices.

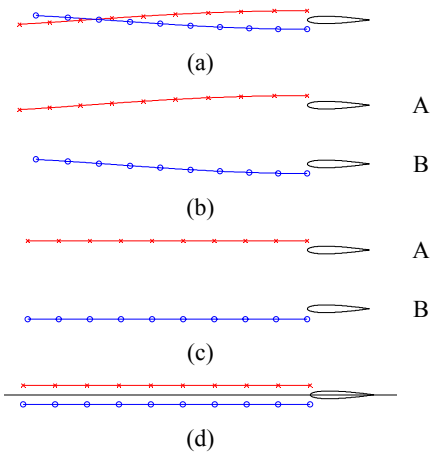

Fig.11 Decomposition of blade-two vortices interaction into two blade-single vortex interactions (a) original case (b) unphysical path (c) modified path to match the same miss-distances (d) summation

initial positions (x, y) (decomposed simulation)	double impinging (-4.5,0.0) (-4.2,0.0) both-sides skimming (-4.5,0.15) (-4.5,-0.15)

Table 3 Simulation conditions for decomposed simulation

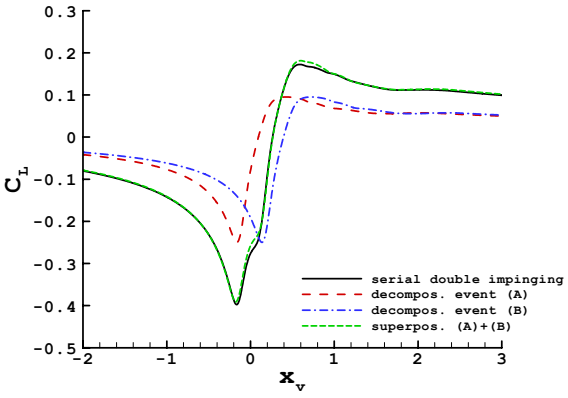

(a)

(continued)

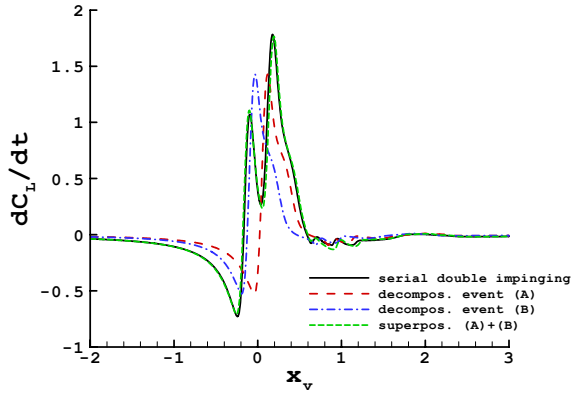

(b)

Fig.13 Aerodynamic fluctuations for *double impinging* case (a) lift (b) time derivative of lift

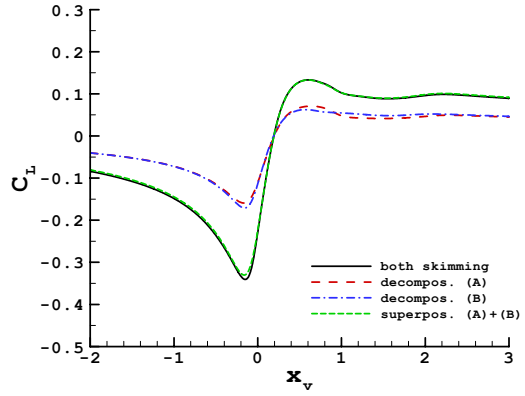

(a)

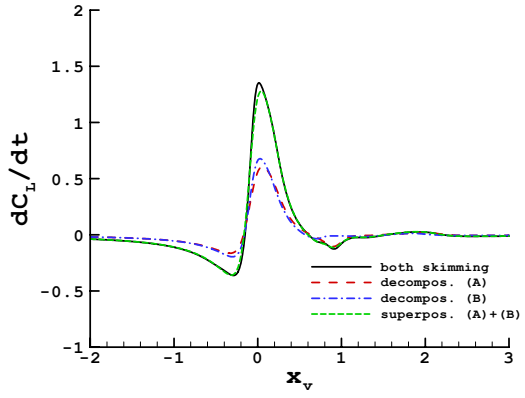

(b)

Fig.14 Aerodynamic fluctuations for *both-sides skimming* (a) lift (b) time derivative of lift

CONCLUSION

Two dimensional BVIs with single vortex and split vortices are studied by using a high order optimized compact scheme. The following conclusions are drawn from this study.

- The importance of miss-distance is emphasized by our simulation results. For interaction of split vortices with blade, aerodynamic fluctuation on the blade surface depends mainly on the miss-distance of each vortex, not the trajectories of co-rotating vortices.

- It was shown that BVI with split-vortices can be decomposed into individual interactions of each vortex with the miss-distance modified by co-rotation of the vortices. It is expected that various configurations of split vortices can be calculated conveniently as individual blade-single vortex interaction.

REFERENCES

1. Brocklehurst, A. and Pike, A.C., Reduction of BVI noise using a vane tip, AHS Aeromechanics Specialists Conference, 1994

2. Beddoes, T.S. and Pike A.C., Noise Reduction with a Twin Tip Vortex Configuration, AHS 52nd Annual Forum, 1996

3. Brand, A.G., Aerodynamic Analysis and Measurement of a Subwing Blade Tip Shape for Blade-Vortex Interaction Noise Reduction, AHS 53rd Annual Forum, 1997

4. Gandhi, F. and Tauszig, L., A Method to Evaluate the Contributions of Individual Interactions to Helicopter Blade-Vortex Interaction Noise, Journal of AHS, Vol. 48, pp. 287-299, 2003

5. Hwang, C. and Joo, G., Parametric Study for the Low BVI Noise BERP Blade – KBERP Design Using DEAF, 27th European Rotorcraft Forum, 2001

6. Kim, J.W. and Lee, D.J., Optimized Compact Finite Difference Schemes with Maximum Resolution, AIAA Journal, Vol. 34, pp. 887-893, 1996

7. Kim, J.W. and Lee. D.J., Generalized Characteristic Boundary Conditions for Computational Aeroacoustics, AIAA J., Vol. 38, pp.2040-2049, 2000

8. Kim, J.W. and Lee, D.J., Adaptive Nonlinear Artificial Dissipation Model for Computational Aeroacoustics, AIAA J., Vol. 39, pp. 810-818, 2001

9. Kim, J.W. and Lee. D.J., Characteristic Interface Conditions for Multiblock High-Order Computation on Singluar Structured Grid, AIAA J., Vol. 41, pp.2341-2348, 2004

10. Lee, D.J., Surface Pressure Fluctuations due to Impinging Vortical Flows upon an Airfoil, AIAA paper 1988-3657, 1988

11. Yu., Y.H., Rotor Blade-Vortex Interaction : Generating Mechanism and its Control Concepts, Progress in Aerospace Science, Vol. 36, pp.97-115, 2000